catalysts

MDPI

Article

Highly Efficient Hydrogenation of Guaiacol over Ru/Al_2O_3-TiO_2 Catalyst at Low Temperatures

Yumeng Song [1], Ping Chen [1], Hui Lou [1,*], Xiaoming Zheng [1] and Xiangen Song [2,*]

[1] Key Laboratory of Applied Chemistry of Zhejiang Province, Institute of Catalysis, Zhejiang University, Hangzhou 310028, China; everfornever@126.com (Y.S.); c224@zju.edu.cn (P.C.)
[2] Dalian National Laboratory for Clean Energy, Dalian Institute of Chemical Physics, Chinese Academy of Sciences, 457 Zhongshan Road, Dalian 116023, China
* Correspondence: hx215@zju.edu.cn (H.L.); xiangensong@dicp.ac.cn (X.S.)

Abstract: In this work, the highly efficient hydrogenation of guaiacol catalyzed by ruthenium supported on Al_2O_3-TiO_2 (Ru/Al_2Ti_1) at very mild conditions was carried out. At temperatures as low as 25 °C and 2 MPa H_2, about 60% of guaiacol could be converted to 2-methoxycyclohexanol (MCH) with a selectivity as high as 94% on the Ru/Al_2Ti_1 catalyst with an appropriate hydrogen pressure. At temperatures above 50 °C, almost all of the guaiacol could be converted with the catalyst of Ru/Al_2Ti_1, mainly into hydrogenated products such as MCH. The surprisingly efficient hydrogenation of guaiacol at low temperatures was most likely due to the ability of Ru particles loaded on the specific complex metal oxide carriers, particularly the reduction of the edge effect of Ru, to activate phenyl and hydrogen and reduce the competition of the dimethoxy process. These findings about the high activity of the Ru/Al_2Ti_1 catalyst at nearly room temperature may be helpful to upgrading the industrial process of the pyrolysis bio-oils.

Keywords: guaiacol; Ru; hydrogenation; bio-oil

Citation: Song, Y.; Chen, P.; Lou, H.; Zheng, X.; Song, X. Highly Efficient Hydrogenation of Guaiacol over Ru/Al_2O_3-TiO_2 Catalyst at Low Temperatures. *Catalysts* **2024**, *14*, 827. https://doi.org/10.3390/catal14110827

Academic Editor: Ivan V. Kozhevnikov

Received: 9 October 2024
Revised: 6 November 2024
Accepted: 11 November 2024
Published: 17 November 2024

1. Introduction

Pyrolysis bio-oil has attracted much attention in recent years as a renewable fuel. As the source of bio-oil, the biomass comprises hemicellulose (typically 25%), cellulose (40–50%), and lignin (15–20%), depending on its original plant species, and could be extensively obtained from lignin and cellulosic biomass [1]. Among them, lignin is significantly different from cellulose and hemicellulose in terms of structure and composition, with high aromaticity and low oxygen content. Therefore, the conversion of the lignin is very difficult, and the related industrial process still needs to be developed. In contrast, the conversion of the cellulosic biomass has been studied a lot in the past, and some mature industrial processes have been realized [2].

Currently, crude bio-oil can be easily obtained from the lignin with a thermal cracking technique. Usually, crude bio-oil is a complex mixture composed of acids, aldehydes, ketones, esters, phenols, carbohydrates, and other substances, and water accounts for about 30%, which cannot be directly applied [3]. Particularly, the phenolic hydroxyl group and acids in the crude bio-oil could cause a polymerization reaction in the phenol oligomers, which seriously hinders its application [4].

Phenolic compounds, including guaiacol, vanillin, and eugenol, which are derived from the lignin, make up about 30 wt. % of the crude bio-oils [5]. It is difficult to find catalysts to efficiently upgrade crude bio-oils into stable fuels because alcohols, ethers, ketones, and esters could affect the effective conversion of phenolic compounds [6].

Some catalysts have been proven to effectively convert the phenolic compounds, but most of them have to be carried out at temperatures over or about 200 °C. However, at a high temperature, phenolic compounds tend to re-polymerize into heavy hydrocarbons and form coke during the conversion process, and high temperatures could result in

the accumulation of carbon deposition during the reaction [7]. Therefore, reducing the reaction temperature is not only economical and helps to save energy, but it is also essential and benefits the reusage of the catalyst. It is of great practical importance to develop catalysts with high activity and selectivity at mild conditions to upgrade crude bio-oils into stable fuels.

As an important model compound of lignin pyrolysis, the catalytic conversion of guaiacol has attracted much attention, especially under mild conditions or at low temperatures [8,9]. Most studies have been aimed at the efficient hydrodeoxygenation of guaiacol, possibly due to the fact that the product could be directly applied.

In order to achieve the efficient hydrodeoxygenation of guaiacol, a variety of catalysts have been studied, such as Ni, Co, Mo, and Fe, and some other noble metals, such as Ru, Pt, Pd, Re, Ag, and Au. Usually, carbon materials, such as activated carbon, carbon nanotubes, carbon nanofibers, and oxides such as SiO_2, ZrO_2, CeO_2, TiO_2, and Al_2O_3, are the main types of supports. Oxide supports could affect the acidity of the catalyst and improve catalytic performance [10]. However, when the reaction system contains water, the stability of the acidic oxides is very important, since the hydrolysis of the oxide surface and other side reactions could break the synergized effect between the noble metal and the oxide surface [11–13]. It has been found that the Al_2O_3 support could be modified with TiO_2, ZrO_2, CeO_2, etc., so that the stability of the catalysts can be increased and the catalytic activity can also be improved [14–17].

Under mild conditions, many studies on the catalytic hydrodeoxygenation of guaiacol have been reported. At 220 °C, Ge et al. [18] could convert guaiacol to cyclohexanol over core–shell Cox@C@Ni catalysts using isopropanol as the H-donor solvent. At 180 °C and 2 MPa H_2 pressure, Lu et al. [19] studied a nanoporous Ni (NP-Ni) catalyst in which 100% conversion of guaiacol and over 90% selectivity to cyclohexanol were achieved with water as the solvent for 4 h. At 150 °C and 0.5 MPa of H_2 pressure, Rong et al. [20] found that guaiacol could be completely converted using an NP-$NiMnO_2$ catalyst. At 1 MPa H_2 and 200 °C, Wu et al. [21] studied a co-modified zeolite (Co/TS-1) catalyst to convert guaiacol with 94.3% efficiency.

In contrast to transition metals, noble metals typically provide an activated H_2 active site and could affect the acidity of the oxide supports, which may improve catalytic performance at mild conditions with less catalyst poisoning. With a Pd/m–MoO_3–P_2O_5/SiO_2 catalyst at 453 K and 1 MPa H_2, Duan et al. [22] could convert guaiacol with the production of 9.4% total mass as liquid alkanes, which involved 0.9% pentane, 1.2% hexane, and 5.6% of cyclohexane, methylcyclohexane, ethylcyclohexane, and propylcyclohexane. Under very low temperatures (<100 °C) and H_2 pressure (<1 atm) and a SiW_{12} and Pt/C catalyst system, Liu et al. [23] obtained high hydrocarbon yields by converting guaiacol.

Compared with traditional noble metals such as Pt and Pd, Ru could be more effective at lower temperatures, and is not as expensive as Pt and Pd, offering good potential for use as a catalyst for the hydrodeoxygenation of guaiacol in mild conditions [24,25]. Gates et al. found that a Ru/Al-HMS catalyst could achieve a quantitative hydrodeoxygenation of guaiacol at conditions of 200 °C and 5 MPa H_2 [26]. Chen et al. [27] reported a Ru-Mn/Al_2O_3-SiO_2 catalyst with 100% guaiacol hydrodeoxygenation at 180 °C and 2 MPa H_2 pressure for 4 h. According to a study by Hu et al. [28], guaiacol could be completely converted to cyclohexane under 180 °C and 3 MPa H_2 pressure on Ru/Hβ (DP) catalysts. Recently, Hyungjoo Kim et al. [29] reported that Ru (5%)/DT-51 achieved 100% conversion with a 36.5% selectivity of cyclohexanol at 100 °C and under low hydrogen pressure with sulfur. However, sulfur-containing catalysts may cause sulfur oxide emission problems, which is not good for environmental protection. It may prevent a follow-up application.

Nearly all of the abovementioned studies for the hydrodeoxygenation of guaiacol were carried out at temperatures of around 200 °C and under certain hydrogen pressures. The efficiency of the catalysts at a low temperature is usually sensitive to hydrogen pressure. Under high hydrogen pressure, the efficiency of the catalyst can often increase. However, high hydrogen pressure could significantly reduce the selectivity of the target product.

Additionally, for bio-oil upgrading, the conversion often has to be carried out at a reasonably high hydrogen pressure [30,31]. Previous studies showed that guaiacol could be converted into many different products with benzene-hydrogenation, alkyl-transform, demethylation, dimethoxylation, and dehydration reactions [32]. The distribution of the products is affected by the catalysts and reaction conditions. Li et al. [33] determined that guaiacol was mainly converted into 1-methyl-1,2-cyclohexanediol with the Ni/CK-800 catalyst at 220 °C and under a hydrogen pressure of 2 MPa. Parrilla-Lahoz et al. [34] found that catechol was the main product at 300 °C with the $NiCeO_2$ catalyst. The high selectivity of cyclohexanol was shown with the catalyst Ni/ZrO_2-CeO_2 at 220 °C and under a hydrogen pressure of 2 MPa [35]. Studies of Mo_2C and Mo/AC catalysts show that phenol and anisole are the main products produced at around 250 °C [36–38]. Furthermore, cyclohexane was the main product in some studies of Ru catalysts, produced at around 300 °C [39–42]. Apparently, catalytic guaiacol conversion under even milder conditions still needs to be developed for the achievement of final industrial production.

In this paper, efficient, catalyzed guaiacol hydrogenation conversion with high selectivity is reported at very low temperatures and under 1 MPa or higher hydrogen pressure, i.e., at temperatures around 50 °C with a catalyst of Ru/Al_2O_3-TiO_2, in which the Al_2O_3-TiO_2 composite oxide supports different Al/Ti ratios prepared by the co-precipitation method, and the highly dispersed 5% Ru/Al_2O_3-TiO_2 bifunctional catalyst was prepared by the impregnation method.

2. Results and Discussion

2.1. Characterization of Catalysts

Figure 1 shows the powder XRD patterns of Ru-catalysts on different supports. Except for Ru/Al_2O_3, all other catalysts had similar diffraction patterns. Four Ru diffraction peaks at 2θ = 42.15, 44.01, 58.31 and 78.38° (JCPDS No. 06-0663) were observed. The others, at 2θ = 25.28, 36.95, 37.80, 38.90, 48.05, 53.89, 55.06, 62.69, 68.76, 70.31 and 75.03°, were attributed to anatase TiO_2 (JCPDS No. 21-1272). As the molar ratios of aluminum to titanium increased from 1:4 to 4:1, no peaks of Al_2O_3 were observed in the XRD patterns, which indicated that Al_2O_3 might exist in a solid solution state with TiO_2, and it also prevented titania from phase transformation (anatase to rutile) [43,44]. The crystal sizes of Ru on TiO_2 and complex oxides calculated from the Scherrer equation were congruous, around 8 nm to 12 nm, in which the crystal size of Ru/Al_2Ti_1 was 9.04 nm. While the crystal size of Ru/Al_2O_3 was up to 13.67 nm, slightly bigger than that of other catalysts, it is consistent with the theory that the structures of complex oxide catalysts were closer to those of TiO_2.

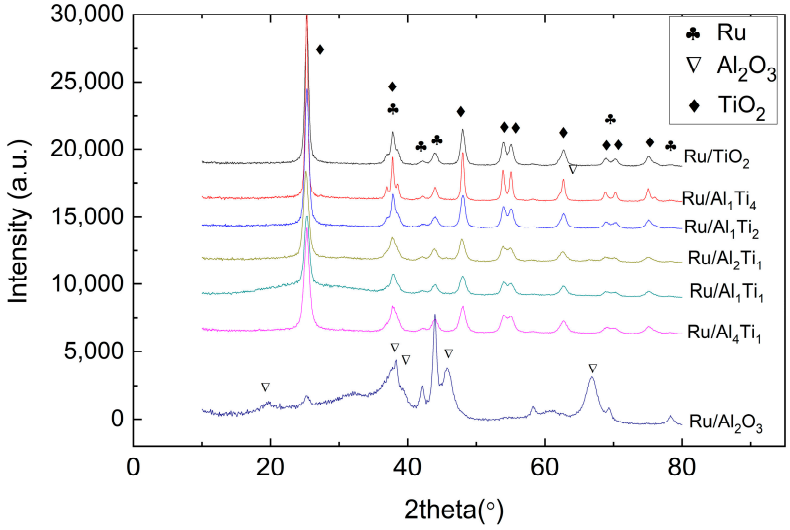

Figure 1. Powder XRD patterns of Ru catalysts on different supports.

The surface areas of the catalysts in BET are listed in Table 1. The specific surface area of Al/Ti composite oxide-supported Ru catalysts ranged from 30 to 100 m^2/g. The proportion of metal elements may significantly affect the specific surface area of the composite oxide [45–48], and even the crystalline phase structure is similar. According to Table 1, the increase in the Al/Ti ratio in complex oxides may result in an increase in the surface area. The surface area may have no significant influence on catalyst activity.

Table 1. BET of Ru catalysts on different supports.

Catalyst	Surface Area/(m^2 g^{-1})
Ru/TiO_2	36
Ru/Al_1Ti_8	35
Ru/Al_1Ti_4	47
Ru/Al_1Ti_2	43
Ru/Al_1Ti_1	58
Ru/Al_2Ti_1	67
Ru/Al_4Ti_1	76
Ru/Al_8Ti_1	105
Ru/Al_2O_3	168

The transmission electron microscopy (TEM) image in Figure 2 shows that metal particles' sizes were congruous, and around 40 nm to 60 nm. Comparing the order of activity of catalysts and surface areas, the surface area size may not be the main factor that determines the activity of the catalyst in this reaction. Therefore, the TEM image is consistent with the crystal sizes according to the XRD results. The hydrogenation of the benzene ring is not sensitive to the sizes of metal particles [49–52]. This may result in the high selectivity of a single product, which is beneficial for the product separation and application of upgrading bio-oil.

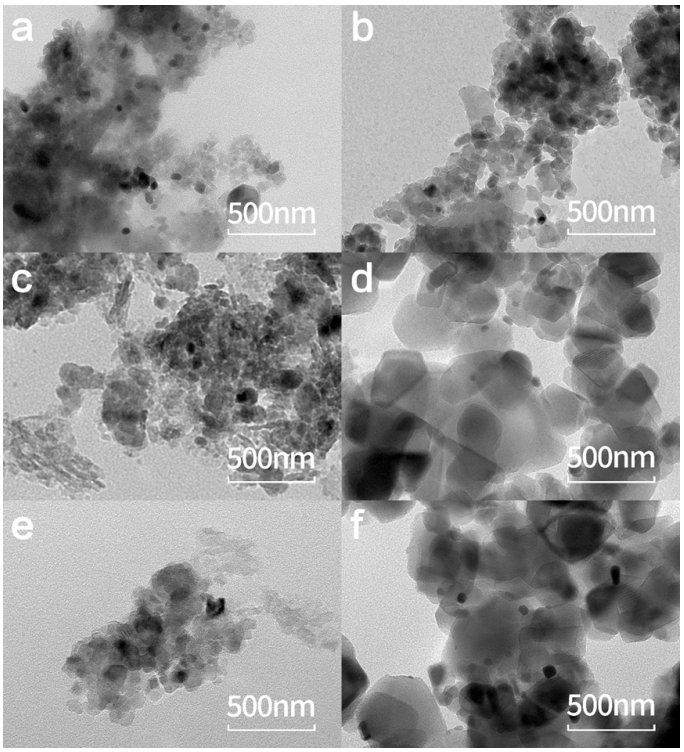

Figure 2. Electron microscopic images of the catalysts. Sample (**a**) for Ru-Al_2Ti_1, sample (**b**) for Ru-Al_2Ti_1 used at 100 °C for 5, sample (**c**) for Ru-Al_2O_3, sample (**d**) for Ru-TiO_2, sample (**e**) for Ru-Al_8Ti_1 and sample (**f**) for Ru-Al_1Ti_8.

The NH_3-TPD profiles of the oxide supports and different supported catalysts of Ru are shown in Figures 3 and 4. The acid amounts of Ru-catalysts on different supports were recorded in Table 2. The desorption temperature of ammonia could roughly be divided into two temperature ranges, indicating weak and strong acidic sites. According to Figure 4, the acid strengths of Al-Ti mixed oxide support and TiO_2 are similar and significantly weaker than that of Al_2O_3. This is consistent with the results of previous studies [53].

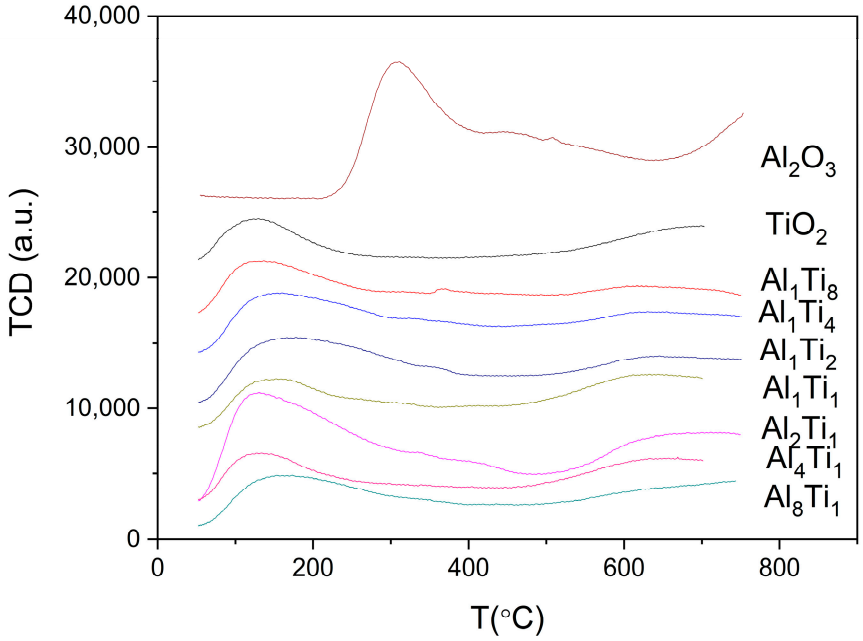

Figure 3. NH_3-TPD of different oxide supports.

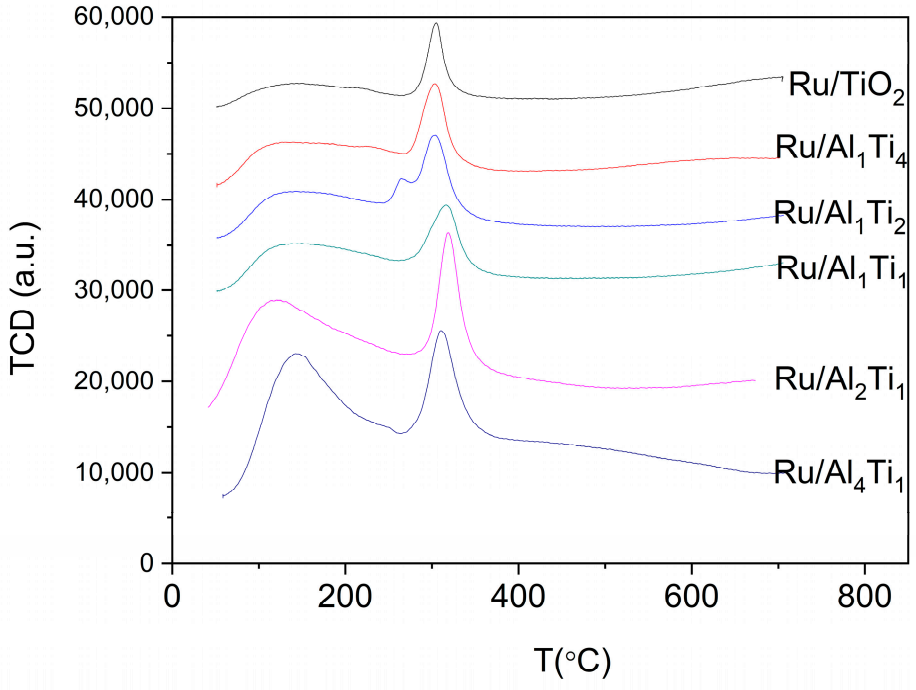

Figure 4. NH_3-TPD of Ru catalysts on different supports.

Table 2. Acid amounts of Ru catalysts on different supports.

Catalysts	Temperature of Ammonia/°C	Acid Amount/(mmol/g)	Temperature of Ammonia/°C	Acid Amount/(mmol/g)
Ru/Al_4Ti_1	136.3	0.194	302.6	0.143
Ru/Al_2Ti_1	125.7	0.320	325.9	0.166
Ru/Al_1Ti_1	139.6	0.126	315.2	0.102
Ru/Al_1Ti_2	138.4	0.089	302.6	0.067
Ru/Al_1Ti_4	125.7	0.075	304.4	0.091
Ru/TiO_2	136.3	0.042	304.4	0.044

The high acid strength activates the C–O bond more easily and affects the electron cloud density of the benzene ring, inhibiting Ru particles' activation of the benzene ring. Low acid strength is beneficial to reducing the formation of carbon deposits, which is an important factor in bio-oil upgrading.

Comparing the results in Figures 3 and 4, the metal particles of Ru provided additional acid sites, where the temperatures of ammonia desorption were around 300 °C. Weak acidic sites with the desorption temperature of ammonia around 130 °C were seen, especially for oxides and Ru supported on Al_2Ti_1. All these results are similar to those derived with TiO_2 oxides. The strengths of the acid sites of Ru/Al_2Ti_1 are slightly stronger. The acid sites may form a synergistic effect with the Ru particles to favor the adsorption of reactant molecules, indicating that a higher amount of acid may be beneficial for the reaction.

The H_2-TPR results of Ru catalysts on different supports are shown in Figure 5. Hydrogen consumptions is listed in Table 3. All reduction temperatures were under 300 °C. Ru-Al_2Ti_1 was observed with the lowest reduction temperature and the greatest hydrogen consumption among the series catalysts. This indicates that the Al doping may affect the support surface, and further form a synergistic effect with Ru particles to enhance the adsorption and activation of Ru particles to H_2.

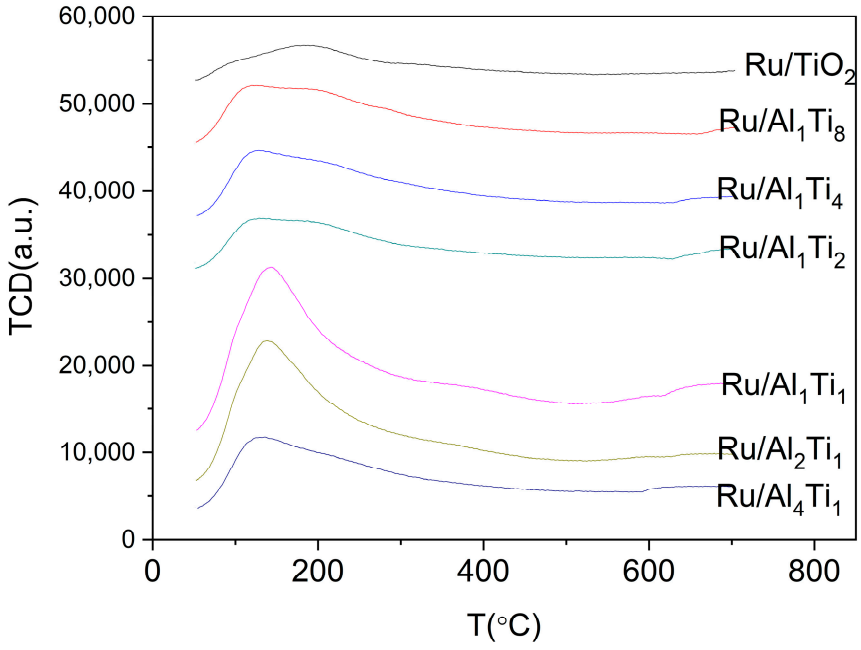

Figure 5. H_2-TPR of Ru catalysts on different supports.

Table 3. H_2-TPR of Ru-catalysts on different supports.

Catalyst	Temperature of Reduction Peak/°C	Peak Area/g
Ru/Al_4Ti_1	129.3	12,800
Ru/Al_2Ti_1	122.2	21,071
Ru/Al_1Ti_1	154.4	19,615
Ru/Al_1Ti_2	158.6	11,386
Ru/Al_1Ti_4	134.7	9830
Ru/TiO_2	189.7	4324

2.2. Catalytic Activities

Table 4 lists the catalytic activities of Ru-supported catalysts on guaiacol conversion at 150 °C and 2 MPa H_2 with 0.02 g of catalysts. As a comparison, the results for a commercial catalyst, Ru/C, were also derived. It can be seen that the guaiacol conversions over Al_2Ti_1-, Al_1Ti_1- and Al_1Ti_2-supported Ru catalysts were higher than others. The highest conversion was obtained from Ru/Al_2Ti_1. Under the reaction conditions of 150 °C and 2 MPa H_2, more than 70% of guaiacol was converted, with a selectivity of more than 95% to hydrogenated species (2-methoxy-cyclohexanol) and less than 5% to hydrodeoxygenated species (cyclohexanol and cyclohexyl methyl ether). Since phenolic substances are the precursors of coke, reducing the content of phenolic hydroxyl groups has a prominent effect on the stability of catalyst and leads to a very good value of bio-oils, which could not be seen in our catalyzed products.

Table 4. Catalytic effects of Ru supported catalysts on guaiacol conversion [1].

Catalyst	Conversion/%	Selectivity/%	
		Hydrogenation	Hydrodeoxygenation
Ru/C	29.2	95.5	4.5
Ru/Al_2O_3	51.4	91.0	9.0
Ru/TiO_2	5.4	100	0
Ru/Al_4Ti_1	30.7	96.2	3.8
Ru/Al_2Ti_1	72.2	96.7	3.3
Ru/Al_1Ti_1	67.1	96.4	3.6
Ru/Al_1Ti_2	67.0	96.2	3.8
Ru/Al_1Ti_4	16.6	33.5	6.5

[1] reaction conditions: 150 °C and 2 MPa H_2 on 0.02 g catalysts.

Anyway, the composition of bio-oil is complex, usually including acids, aldehydes, ketones, esters, phenols, carbohydrates, etc., and their distribution varies greatly according to the different sources and production processes. These components in the mixture will be subjected to many different chemical reactions, including hydrogenation, cracking, isomerization, and esterification. It is good to see that the main product, 2-methoxycyclohexanol, could impart stability in the follow-up catalyst, and there is no esterification or etherification with other components of crude bio-oil, such as acids and alcohols. The Ru supported on Al_2Ti_1 catalysts with high conversion and selectivity might have a good applicability.

Table 5 shows the guaiacol conversions and product selectivity obtained over Ru/Al_2Ti_1 at different temperatures. From 50 to 150 °C, almost all of guaiacol was converted, mainly to hydrogenated products and 2-methoxycyclohexanol. Even when the reaction temperature was lower than 25 °C, about 60% of guaiacol was still converted to 2-methoxycyclohexanol with a selectivity of 94%. As the temperature increased from 25 to 150 °C, the selectivity of hydrogenation decreased slightly from 94% to 77%, while hydrodeoxygenation selectivity increased from 6% to 23%. Obviously, a lower temperature favored hydrogenation, while higher temperatures were conducive to hydrodeoxygenation [50]. In the current study, the

hydrogenation reaction temperature of guaiac was around 150–200 °C. Guaiacol was nearly completely converted by Ru/Al_2Ti_1 at 50 °C, which temperature is significantly lower than the 100 °C reported by Hyungjoo Kim et al. [28].

Table 5. Guaiacol conversion over Ru/Al_2Ti_1 at different reaction temperatures [1].

T/°C	Conversion/%	Selectivity/%	
		Hydrogenation	Deoxidation
25	59.5	94.1	5.9
50	97.2	88.9	11.1
100	100	89.0	11.0
150	100	76.5	23.5

[1] reaction condition: 0.1 g catalyst, 2 MPa H_2, 3 h.

The transformation pathway of guaiacol is schematically shown in Figure 6. Phenyl hydrogenation and dimethoxy are the two main transformation steps. A schematic diagram of guaiacol transformation on the catalyst surface is shown in Figure 7. The adsorption and activation of phenyl and hydrogen mainly occur on the surface of the Ru metal particles, while the activation of the methoxy group mainly occurs on the surface of the oxide carrier, and the deoxidation reaction requires the synergistic action of the metal particles and the oxide support.

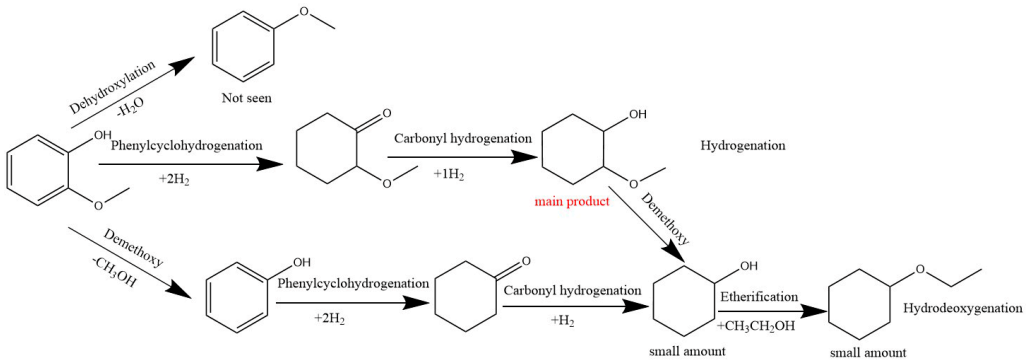

Figure 6. Conversion of guaiacol by Ru supported on oxides.

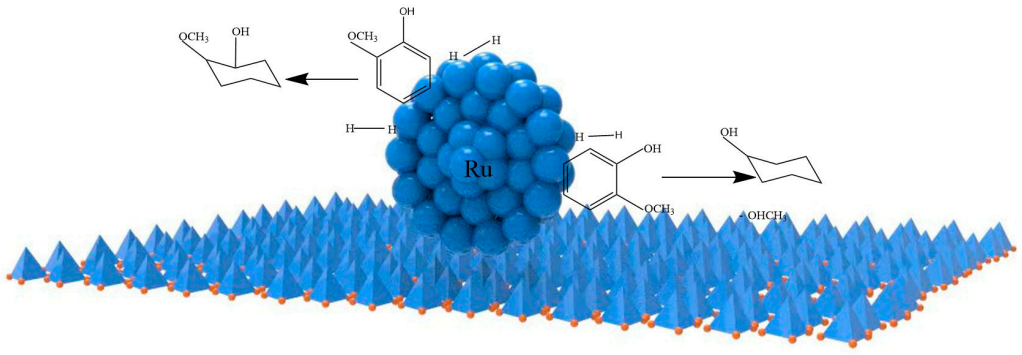

Figure 7. Schematic diagram of the catalyst's surface.

The C_{ring}-O bond cleavage has a strong temperature dependence related to the Gibbs free energy [5156]. Therefore, as the temperature increases, the rate of the dimethoxy process could be made faster than that of the hydrogenation process, resulting in an increase in the competitiveness of the deoxygenation reaction, which is the most important competitive reaction in the studied reaction system. This may explain the high selectivity of the deoxidation product.

It is well known that most of the lignin in biomass would be converted to phenols, guaiacols and anisole during pyrolysis. These lignin-derived compounds make up about 30 wt. % of bio-oils, and they tend to be repolymerized to produce heavy hydrocarbons and coke during the upgrading process at high temperatures, even in storage [5257]. Therefore, the high activity of the Ru/Ai-Ti catalyst at nearly ambient temperature is very advantageous for upgrading pyrolysis bio-oil.

The results of the guaiacol conversion over Ru/Al_2Ti_1 at different hydrogen pressures are shown in Table 6. In the range of 0.1 MPa to 1 MPa, the conversion rate increases gradually with the increase in hydrogen pressure, and the conversion reaches 99% at 1 MPa. With the increase in hydrogen pressure, the selectivity of hydrogenation products increases and the selectivity of deoxidation products decreases. Dimethoxy and phenyl hydrogenation are competing processes, as shown in Figure 6. The hydrogenation reaction mainly occurs on metal particles. High hydrogen pressure will increase the rate of the hydrogenation process, and the hydrogenation of the benzene ring will further inhibit the dimethoxy-process [5358]. Therefore, as the hydrogen pressure increases, the selectivity of 2-methoxycyclohexanol rises. As seen in Table 6, the catalyst has a high catalytic efficiency with a high selectivity in a wide range of hydrogen pressures, which significantly benefits the upgrading of bio-oils.

Table 6. Guaiacol conversion over Ru/Al_2Ti_1 at different hydrogen pressures [1].

Hydrogen Pressure/MPa	Conversion/%	Selectivity/%	
		Hydrogenation	Deoxidation
0	1.8	100	0
0.1	68.6	63.8	36.2
0.6	81.6	70.3	29.7
1	99.1	81.1	19.9
2	100	89.0	11.0
4	100	91.7	8.3

[1] reaction condition: 0.1 g catalyst, 100 °C, 3 h.

The guaiacol conversion variations at different reaction times were also examined, and the results are shown in Figure 8. At 100 °C, the conversion was stable after 90 min, at close to 100%, while at 50 °C, the conversion was stable at 97% after 210 min. This is obviously related to the reduction of ruthenium, since a higher reaction temperature is beneficial to the reduction of Ru.

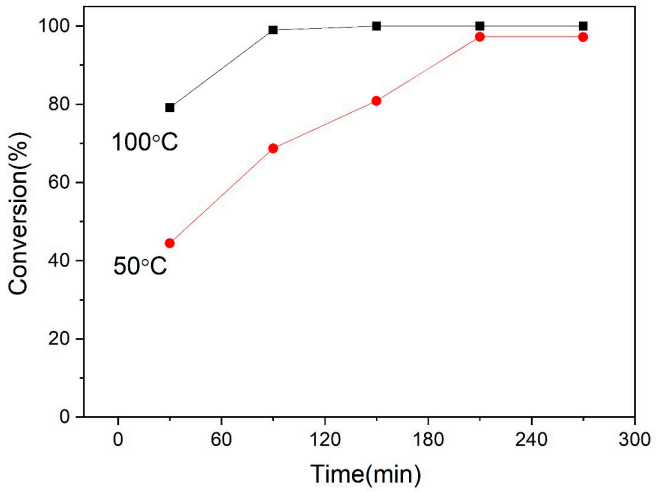

Figure 8. Guaiacol conversion over Ru/Al_2Ti_1 at different reaction times. Reaction condition: 0.1 g catalyst, 50 °C and 100 °C, 2 MPa H_2.

The catalytic hydrogenation results of other bio-oil model compounds over Ru/Al2Ti1 are listed in Table 7. The catalysts also have a good catalytic hydrogenation effect on other phenolic substances commonly found in bio-oil. Similarly, the conversion of phenolic substances reached more than 90% at 100 °C, which may provide a basis for a study on the quality improvement of the bio-oil, even under mild conditions.

Table 7. Conversions of other lignin model compounds [1].

Reagent	Conversion/%	Selectivity/%	
		Hydrogenation	Deoxidation
Phenol	100	100	-
O-methyl-phenol	100	97.4	2.6
Anisole	97.5	100	-
Vanillin	93.7	91.6	8.4
Catechol	92.7	95.6	4.4

[1] reaction condition: 0.1 g catalyst, 100 °C, 2 MPa H_2.

2.3. Catalyst Stability

After reusing it five times, the conversion of guaiacol by use of the Ru/Al_2Ti_1 catalyst has been recorded in Figure 9. It can be seen that the conversion of guaiacol was maintained at 40–50%, which suggests the good stability of the catalytic efficiency.

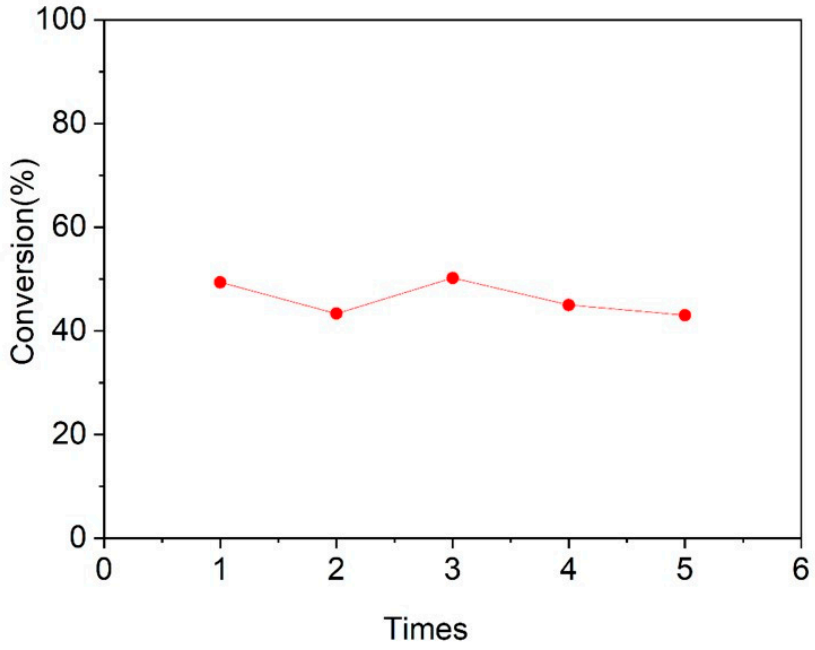

Figure 9. Conversion of Ru/Al2Ti1 catalyst after 5 reuses (reaction condition: 0.03 g catalyst, 100 °C, 2 MPa H_2).

By comparing Figures 2a and 2b, the metal particle sizes did not change significantly after the reaction. Figure 10 shows that the XRD image of the catalyst remained unchanged before and after multiple reactions, and the intensity of the Ru characteristic peak did not decrease. The crystal size of Ru calculated using the Scherrer equation was 9.04 nm and 8.96 nm for fresh and reused catalysts, respectively, indicating that the structure of the catalyst was relatively stable after five repetitions of the reaction. The variations in the sizes of the Ru particles could lead to the instability of catalytic efficiency, caused by aggregation or disintegration, which is more prominent in a high-distribution system of small nanoparticle catalysts. The homogeneous and appropriately large sizes of Ru particles may contribute to the stability of the catalytic performance. In TG tests, we

mainly investigated the carbon deposition of the catalyst and the adsorption of reactants or products. In Figure 11, we see that the weight loss of fresh and spent catalysts is about 1% at about 280 °C, and there is no obvious difference in the catalysts before and after the reaction, indicating that the carbon deposition of the catalyst is not obvious. The morphology and catalytic performance of the catalyst are stable, offering benefits for recycling.

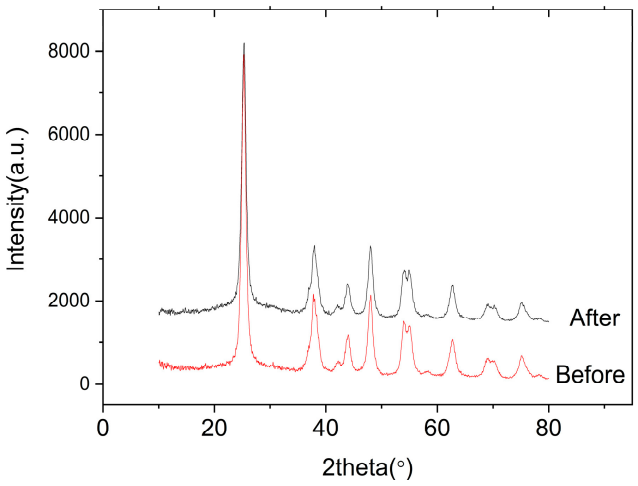

Figure 10. XRD of reused Ru/Al_2Ti_1 catalyst Catalyst used in catalytic conversion at 100 °C 5 times then washed with ethanol 3 times, labeled as After, compared with catalyst washed in ethanol at 100 °C for 3 h, labeled as Before.

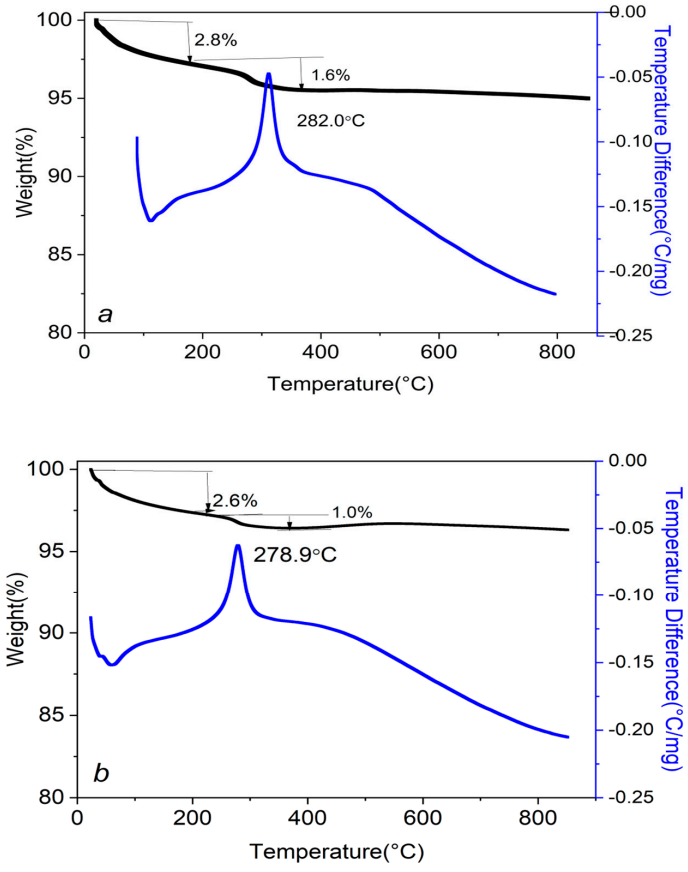

Figure 11. TG of reused Ru/Al_2Ti_1 catalyst. (**a**) shows a catalyst used in catalytic conversion at 100 °C 5 times, then washed with ethanol. (**b**) shows a catalyst in ethanol at 100 °C for 3 h.

3. Materials and Methods

3.1. Materials

Al $(NO_3)_3 \cdot 9H_2O$ (99.99% metals basis) and $RuCl_3 \cdot xH_2O$ (Ru% 35–42%) were purchased from Aladdin Reagents Co., Ltd., Shanghai, China. $TiCl_4$ (CP), absolute ethanol, phenol, anisole, vanillin, catechol, 2-methylphenol and guaiacol were purchased from Sinopharm Chemical Reagent Co., Ltd., Beijing, China. All chemicals were obtained commercially and used without further treatment.

3.2. Catalysts Preparation

The alumina and titania composite oxides were prepared by the precipitation method. Firstly, predetermined quantities of Al $(NO_3)_3 \cdot 9H_2O$ and $TiCl_4$ were mixed in Al/Ti molar ratios of 1/8, 1/4, 1/2, 1/1, 2/1, 4/1, and 8/1, respectively, and then dissolved completely in deionized water to form a solution. The excess ammonium hydroxide was then added to the solution under continuous stirring until the pH value reached 9, and we then kept stirring at pH = 9 and 40 °C for 4 h. An aluminum and titanium hydroxides precipitate formed, which was washed with deionized water until reaching a neutral solution. After being dried overnight at 100 °C, it was calcined in air at 550 °C for 3 h. The obtained oxides with different alumina and titania molar ratios were denoted as Al_xTi_y. The ratio of Al and Ti was based on the amount of materials, and the productivities of all composite oxides were above 95%.

The 5% Ru-supported catalysts were prepared by incipient wetness impregnation with $RuCl_3$ aqueous solution. Impregnation was followed by calcination in air at 300 °C for 1 h and reduction by H_2 at 400 °C for 3 h, respectively.

3.3. Catalysts Characterization

The Brunauer–Emmett–Teller (BET) surface areas of the supports were obtained by N_2 physisorption with a Micrometritics ASAP 2000 automated system. X-ray diffraction patterns (XRD) of the supports and the catalysts were acquired on a RIGAKU D/MAX 2550/PC diffractometer in the scan range of 10° to 80°, using Cu Ka1 radiation (k = 1.540 56 Å) at 40 kV and 30 mA. The power diffraction file (PDF) database was used to determine the phase of the materials. The temperature-programmed desorption of NH_3 (NH_3-TPD) was used to test the acidity of the materials. The samples were firstly pretreated in flowing nitrogen at 450 °C for 1 h, cooled down to 50 °C, adsorbed with NH_3 for 1 h, flushed with helium (50 mL/min) for 1 h to remove NH_3 in the gas phase and in the physisorpted state, and then the temperature was raised to 750 °C with a heating rate of 10 °C/min while TPD profiles were recorded.

Hydrogen temperature programmed reduction (H_2-TPR) was used to determine the reduction temperature and reducibility of the catalyst. Samples were pretreated in a helium gas flow at 450 °C for 30 min, which was cooled to 50 °C. After the chromatographic baseline was stabilized, the sample was heated to 700 °C at a rate of 10 °C/min in TPR gas (5% H_2 in N_2). Thermogravimetric (TG) assessment was performed under an air atmosphere with a heating rate of 10 °C/min from 20 °C to 800 °C. The morphology and structure of the catalyst surface and the particle size and dispersion of the supported metal were characterized by electron microscopy. The TEM acceleration voltage was 300 kV.

3.4. Catalytic Activity Measurement

In a typical catalytic reaction, 0.1 g substrate, 15 mL ethanol and a certain amount of catalyst were added into a 30 mL stainless sealed constant temperature reactor. After exchanging air with H_2 4 times, the system was pressured with H_2 to 2 MPa and sealed. Then, it was heated to the set reaction temperature and kept for 3 h with stirring at 600 rpm.

For the catalyst stability tests, the spent catalyst was collected, washed with ethanol three times, dried at 100 °C for 2 h, and then reused under the same reaction conditions.

3.5. Products Analysis

The reaction product in the liquid phase was obtained by filtrating to separate from the catalyst after cooling the reactor to room temperature. It was analyzed qualitatively through a gas chromatography–mass spectrometer (GC-MS, QP2010SE, Shimadzu Ltd., Kyoto, Japan) equipped with a Rxi-5Sil MS capillary column (30 m × 0.2 m × 0.25 μm) and quantitatively through a GC equipped with a flame ionization detector (FID) and an HP-5 fused silica capillary column (30 m × 0.25 mm × 0.25 μm). Benzyl alcohol was used as an inner-standard in the quantification.

4. Conclusions

The highly efficient hydrogenation of the guaiacol was obtained over a catalyst of Ru/Al*x*Ti*y* at low temperatures. With the catalysis of Ru/Al_2Ti_1, almost all of the guaiacol could be converted to hydrogenated products and 2-methoxycyclohexanol at 50 to 150 °C, with 1 MPa or higher hydrogen pressure. Even when the reaction temperature was as low as 25 °C, about 60% of the guaiacol could be converted to 2-methoxycyclohexanol with a selectivity of 94% and with 2 MPa hydrogen pressure, which has significant advantages at lower temperatures compared to the results of current research on guaiacol hydrogenation. Lower temperatures and higher hydrogen pressure favor the formation of 2-methoxycyclohexanol in the conversion. The catalyst is stable for the process and could be recycled at least 5 times. The high efficiency and high selectivity of the Ru/Al_2Ti_1 catalyst for guaiacol conversion at near-room temperature is promising for use in upgrading pyrolysis bio-oil.

Author Contributions: Conceptualization, X.Z.; methodology, H.L.; software, P.C.; validation, Y.S.; formal analysis, Y.S.; investigation, Y.S.; writing—original draft preparation, Y.S.; writing—review and editing, X.S. All authors have read and agreed to the published version of the manuscript.

Funding: This research received no external funding.

Data Availability Statement: Data will be available on request.

Acknowledgments: This work was financially supported by the National Key Research and Development %Program of China (No. 2018YFB1501402).

Conflicts of Interest: The authors declare no conflicts of interest.

References

1. Akhtar, J.; Amin, N.A.S. A review on process conditions for optimum bio-oil yield in hydrothermal liquefaction of biomass. *Renew. Sust. Energy Rev.* **2011**, *15*, 1615–1624. [CrossRef]
2. Sun, Z.H.; Bottari, G.; Afanasenko, A.; Stuart, M.C.A.; Deuss, P.J.; Fridrich, B.; Barta, K. Complete lignocellulose conversion with integrated catalyst recycling yielding valuable aromatics and fuels. *Nat. Catal.* **2018**, *1*, 82–92. [CrossRef]
3. Branca, C.; Giudicianni, P.; Blasi, C.D. GC/MS Characterization of Liquids Generated from Low-Temperature Pyrolysis of Wood. *Ind. Eng. Chem. Res.* **2003**, *42*, 3190–3202. [CrossRef]
4. Bai, X.L.; Kim, W.H.; Brown, R.C.; Dalluge, E.; Hutchinson, C.; Lee, Y.J.; Dalluge, D. Formation of phenolic oligomers during fast pyrolysis of lignin. *Fuel* **2014**, *128*, 170–179. [CrossRef]
5. Czernik, S.; Bridgwater, A.V. Overview of Applications of Biomass Fast Pyrolysis Oil. *Energy Fuels* **2004**, *18*, 590–598. [CrossRef]
6. Ragauskas, A.J.; Williams, C.K.; Davison, B.H.; Britovsek, G.; Cairney, J.; Eckert, C.A.; Frederick, W.J.; Hallett, J.P.; Leak, D.J.; Liotta, C.L.; et al. The path forward for biofuels and biomaterials. *Science* **2006**, *311*, 484–489. [CrossRef]
7. Wang, Y.X.; He, T.; Liu, K.T.; Wu, J.H.; Fang, Y.M. From biomass to advanced bio-fuel by catalytic pyrolysis/hydro-processing: Hydrodeoxygenation of bio-oil derived from biomass catalytic pyrolysis. *Bioresour. Technol.* **2012**, *108*, 280–284. [CrossRef]
8. Kim, H.; Park, J.H.; Ha, J.M.; Kim, D.H. Effect of Hydrogen Spillover on the Ru/TiO_2-Catalyzed Guaiacol Hydrodeoxygenation: Rutile vs Anatase TiO_2. *Catalysis* **2023**, *13*, 11857–11870. [CrossRef]
9. Li, C.Z.; Zhao, X.C.; Wang, A.Q.; Huber, G.W.; Zhang, T. Catalytic Transformation of Lignin for the Production of Chemicals and Fuels. *Chem. Rev.* **2015**, *115*, 11559–11624. [CrossRef]
10. Liang, J.; Li, X.M.; Yu, Z.G.; Zeng, G.M.; Luo, Y.; Jiang, L.B.; Yang, Z.X.; Qian, Y.Y.; Wu, H.P. Amorphous MnO_2 Modified Biochar Derived from Aerobically Composted Swine Manure for Adsorption of Pb (II) and Cd (II). *ACS Sustain. Chem. Eng.* **2017**, *5*, 8824–8835. [CrossRef]
11. Ravenelle, R.M.; Copeland, J.R.; Van Pelt, A.H.; Crittenden, J.C.; Sievers, C. Stability of Pt/γ-Al_2O_3 Catalysts in Model Biomass Solutions. *Top. Catal.* **2012**, *55*, 162–174. [CrossRef]

12. Ravenelle, R.M.; Copeland, J.R.; Kim, W.G.; Crittenden, J.C.; Sievers, C. Structural Changes of γ-Al_2O_3-Supported Catalysts in Hot Liquid Water. *ACS Catal.* **2011**, *1*, 552–561. [CrossRef]
13. Duana, J.; Kima, Y.T.; Lou, H.; Huber, G.W. Hydrothermally stable regenerable catalytic supports for aqueous-phase conversion of biomass. *Catal. Today* **2014**, *234*, 66–74. [CrossRef]
14. Shah, M.; Bordoloi, A.; Nayak, A.K.; Mondal, P. Effect of Ti/Al ratio on the performance of Ni/TiO_2-Al_2O_3 catalyst for methane reforming with CO_2. *Fuel Process. Technol.* **2019**, *192*, 21–35. [CrossRef]
15. Liu, Z.; Cheng, L.J.; Xin, H.U.; Yuan, S.L.; Jiang, Y. Effect of Mg modification on the catalytic performance of Co/γ-Al_2O_3-TiO_2 in the combustion of propane. *J. Fuel Chem. Technol.* **2020**, *48*, 867–874. [CrossRef]
16. Herbert, J.; Santes, V.; Cortez, M.T.; Zárate, R.; Díaz, L. Catalytic hydrotreating of heavy gasoil FCC feed over a NiMo/γ-Al_2O_3-TiO_2 catalyst: Effect of hydrogen sulfide on the activity. *Catal. Today* **2005**, *107–108*, 559–563. [CrossRef]
17. Wang, R.; Chen, L.; Zhang, X.; Zhang, Q.; Li, Y.; Wang, C.; Ma, L. Conversion of levulinic acid to γ-valerolactone over Ru/Al_2O_3–TiO_2 catalyst under mild conditions. *RSC Adv.* **2018**, *8*, 40989–40995. [CrossRef]
18. Ge, F.; Xia, H.H.; Li, J.; Yang, X.H.; Zhou, M.H.; Jiang, J.C. Selective hydrodeoxygenation of guaiacol to cyclohexanol over core-shell Cox@C@Ni catalysts under mild condition. *Fuel Process. Technol.* **2023**, *245*, 107729. [CrossRef]
19. Lu, J.Q.; Liu, X.; Yu, G.Q.; Lv, J.K.; Rong, Z.M.; Wang, M.; Wang, Y. Selective Hydrodeoxygenation of Guaiacol to Cyclohexanol Catalyzed by Nanoporous Nickel. *Catal. Lett.* **2020**, *150*, 837–848. [CrossRef]
20. Rong, Z.M.; Lu, J.Q.; Yu, G.Q.; Li, J.J.; Wang, M.; Zhang, S.F. Promoting selective hydrodeoxygenation of guaiacol over amorphous nanoporous $NiMnO_2$. *Catal. Commun.* **2020**, *140*, 105987. [CrossRef]
21. Wu, L.Z.; Wie, J.H.; Zhang, Y.; He, Y.S.; Wang, X.F.; Guo, H.Q.; Tang, Y.; Tan, L. The selective hydrodeoxygenation of guaiacol to cyclohexanol over cobalt-modified TS-1 catalysts. *Micropor. Mesopor. Mat.* **2023**, *348*, 112347. [CrossRef]
22. Duan, H.H.; Dong, J.C.; Gu, X.R.; Peng, Y.K.; Chen, W.X.; Issariyakul, T.; Myers, W.K.; Li, M.J.; Yi, N.; Kilpatrick, A.F.R.; et al. Hydrodeoxygenation of water-insoluble bio-oil to alkanes using a highly dispersed Pd–Mo catalyst. *Nat. Commun.* **2017**, *8*, 591. [CrossRef] [PubMed]
23. Liu, W.; You, W.Q.; Sun, W.; Yang, W.S.; Korde, A.; Gong, Y.T.; Deng, Y.L. Ambient-pressure and low-temperature upgrading of lignin bio-oil to hydrocarbons using a hydrogen buffer catalytic system. *Nat. Energy* **2020**, *5*, 759–767. [CrossRef]
24. Ahorsu, R.; Constanti, M.; Medina, F. Recent Impacts of Heterogeneous Catalysis in Biorefineries. *Ind. Eng. Chem. Res.* **2021**, *60*, 18612–18626. [CrossRef]
25. Gao, D.N.; Schweitzer, C.; Hwang, H.T.; Varma, A. Conversion of Guaiacol on Noble Metal Catalysts: Reaction Performance and Deactivation Studies. *Ind. Eng. Chem. Res.* **2014**, *53*, 18658–18667. [CrossRef]
26. Roldugina, E.A.; Naranov, E.R.; Maximov, A.L.; Karakhanov, E.A. Hydrodeoxygenation of guaiacol as a model compound of bio-oil in methanol over mesoporous noble metal catalysts. *Appl. Catal. A Gen.* **2018**, *553*, 24–35. [CrossRef]
27. Chen, M.T.; Zhong, Q.F.; Zhang, M.H.; Huang, H.; Liu, Y.X.; Wei, Z.J. Aqueous phase partial hydrodeoxygenation of lignin-derived phenols over Al_2O_3-SiO_2 microspheres supported RuMn multifunctional catalyst: Synergic effect among Ru, Mn and Al_2O_3-SiO_2 support. *Catal. Commun.* **2022**, *172*, 106550. [CrossRef]
28. Hu, L.; Wei, X.Y.; Zong, Z.M. Ru/Hβ catalyst prepared by the deposition-precipitation method for enhancing hydrodeoxygenation ability of guaiacol and lignin-derived bio-oil to produce hydrocarbons. *J. Energy Inst.* **2021**, *97*, 48–57. [CrossRef]
29. Kim, H.; Yang, S.; Lim, Y.H.; Park, J.H.; Ha, J.-M.; Kim, D.H. Enhanced oxygen removal ability of sulfur-doped Ru/TiO2 catalyst in low-temperature hydrodeoxygenation of guaiacol. *Appl. Catal. A Gen.* **2023**, *661*, 119237. [CrossRef]
30. Stas, M.; Chudoba, J.; Kubicka, D.; Blazek, J.; Pospísil, M. Petroleomic Characterization of Pyrolysis Bio-oils: A Review. *Energy Fuels* **2017**, *31*, 10283–10299. [CrossRef]
31. Prabhudesai, V.S.; Gurrala, L.; Vinu, R. Catalytic Hydrodeoxygenation of Lignin-Derived Oxygenates: Catalysis, Mechanism, and Effect of Process Conditions. *Energy Fuels* **2022**, *36*, 1155–1188. [CrossRef]
32. Blanco, E.; Aguirre, A.D.A.; de León, J.N.D.; Escalona, N. Relevant aspects of the conversion of guaiacol as a model compound for bio-oil over supported molybdenum oxycarbide catalysts. *New J. Chem.* **2020**, *44*, 12027–12035. [CrossRef]
33. Li, T.; Li, H.; Huang, G.M.; Shen, X.R.; Wang, S.Q.; Li, C.L. Transforming biomass tar into a highly active Ni-based carbon-supported catalyst for selective hydrogenation-transalkylation of guaiacol. *J. Anal. Appl. Pyrol.* **2020**, *153*, 104976–104983. [CrossRef]
34. Parrilla-Lahoz, S.; Jin, W.; Pastor-Pérez, L.; Alvarado, D.C.; Odriozola, J.A.; Dongil, A.B.; Reina, T.R. Guaiacol hydrodeoxygenation in hydrothermal conditions using N-doped reduced graphene oxide (RGO) supported Pt and Ni catalysts: Seeking for economically viable biomass upgrading alternatives. *Appl. Catal. A Gen.* **2021**, *611*, 117977–117986. [CrossRef]
35. Lu, M.H.; Jiang, Y.J.; Sun, Y.; Zhang, P.; Zhu, J.; Li, M.S.; Shan, Y.H.; Shen, J.Y.; Song, C.S. Hydrodeoxygenation of Guaiacol Catalyzed by ZrO_2–CeO_2-Supported Nickel Catalysts with High Loading. *Energy Fuels* **2020**, *34*, 4685–4692. [CrossRef]
36. Moreira, R.; Ochoa, E.; Pinilla, J.L.; Portugal, A.; Suelves, I. Liquid-Phase Hydrodeoxygenation of Guaiacol over Mo_2C Supported on Commercial CNF. Effects of Operating Conditions on Conversion and Product Selectivity. *Catalysts* **2018**, *8*, 127. [CrossRef]
37. Ochoa, E.; Torres, D.; Moreira, R.; Pinilla, J.L.; Suelves, I. Carbon nanofiber supported Mo_2C catalysts for hydrodeoxygenation of guaiacol: The importance of the carburization process. *Appl. Catal. B Environ.* **2018**, *239*, 463–474. [CrossRef]
38. Ansaloni, S.; Russo, N.; Pirone, R. Hydrodeoxygenation of guaiacol over molybdenum-based catalysts: The effect of support and the nature of the active site. *Can. J. Chem. Eng.* **2017**, *95*, 1730–1744. [CrossRef]

39. Kim, M.; Ha, J.; Lee, K.; Jae, J. Catalytic transfer hydrogenation/hydrogenolysis of guaiacol to cyclohexane over bimetallic RuRe/C catalysts. *Catal. Commun.* **2016**, *86*, 113–118. [CrossRef]
40. Lin, B.Q.; Li, R.X.; Shu, R.Y.; Wang, C.; Yuan, Z.Q.; Liu, Y.; Chen, Y. Synergistic effect of highly dispersed Ru and moderate acid site on the hydrodeoxygenation of phenolic compounds and raw bio-oil. *J. Energy Inst.* **2020**, *93*, 847–856. [CrossRef]
41. Maity, S.K.; Ancheyta, J.; Llanos, M.E. Alumina–titania binary mixed oxide used as support of catalysts for hydrotreating of Maya heavy crude. *Appl. Catal. A Gen.* **2003**, *244*, 141–153. [CrossRef]
42. Jung, Y.S.; Kim, D.W.; Kim, Y.S.; Park, E.K.; Baeck, S.H. Synthesis of alumina–titania solid solution by sol–gel method. *J. Phys. Chem. Solids* **2008**, *69*, 1464–1467. [CrossRef]
43. Alejandre, A.; Medina, F.; Salagre, P.; Correig, X.; Sueiras, J.E. Preparation and Study of Cu-Al Mixed Oxides via Hydrotalcite-like Precursors. *Chem. Mater.* **1999**, *11*, 939–948. [CrossRef]
44. Debasis, D.; Panchanan, P. Particle Size Comparison of Soft-Chemically Prepared Transition Metal (Co, Ni, Cu, Zn) Aluminate Spinels. *J. Am. Ceram. Soc.* **2006**, *89*, 1014–1021. [CrossRef]
45. Tran, Q.K.; Han, S.; Ly, H.V.; Kim, S.S.; Kim, J. Hydrodeoxygenation of a bio-oil model compound derived from woody biomass using spray-pyrolysis-derived spherical g-Al_2O_3-SiO_2 catalysts. *J. Ind. Eng. Chem.* **2020**, *92*, 243–251. [CrossRef]
46. Newman, C.; Zhou, X.; Goundiea, B.; Ghampson, I.T.; Pollock, R.A.; Ross, Z.; Wheeler, M.C.; Meulenberg, R.W.; Austina, R.N.; Frederick, B.G. Effects of support identity and metal dispersion in supported ruthenium hydrodeoxygenation catalysts. *Appl. Catal. A Gen.* **2014**, *477*, 64–74. [CrossRef]
47. Wachs, I.E. Recent conceptual advances in the catalysis science of mixed metal oxide catalytic materials. *Catal. Today* **2005**, *100*, 79–94. [CrossRef]
48. Wawrzetz, A.; Peng, B.; Hrabar, A.; Jentys, A.; Lemonidou, A.A.; Lercher, J.A. Towards understanding the bifunctional hydrodeoxygenation and aqueous phase reforming of glycerol. *J. Catal.* **2010**, *269*, 411–420. [CrossRef]
49. Teles, C.A.; Magalhães de Souza, P.; Rabelo-Neto, R.C.; Teran, A.; Jacobs, G.; Resasco, D.E.; Noronha, F.B. Hydrodeoxygenation of Lignin-Derived Compound Mixtures on Pd-Supported on Various Oxides. *ACS Sustain. Chem. Eng.* **2021**, *9*, 12870–12884. [CrossRef]
50. Bjelić, A.; Grilc, M.; Likozar, B. Catalytic hydrogenation and hydrodeoxygenation of lignin-derived model compound eugenol over Ru/C: Intrinsic microkinetics and transport phenomena. *Chem. Eng. J.* **2018**, *333*, 240–259. [CrossRef]
51. Hong, J.M.; Prawer, S.; Murphy, A.B. Plasma Catalysis as an Alternative Route for Ammonia Production: Status, Mechanisms, and Prospects for Progress. *ACS Sustain. Chem. Eng.* **2018**, *6*, 15–31. [CrossRef]
52. Mei, Y.; Chai, M.; Shen, C.; Liu, B.; Liu, R. Effect of methanol addition on properties and aging reaction mechanism of bio-oil during storage. *Fuel* **2019**, *244*, 499–507. [CrossRef]
53. Shivhare, A.; Wang, L.; Scott, R.W.J. solation of Carboxylic Acid-Protected Au25 Clusters Using a Borohydride Purification Strategy. *Langmuir* **2015**, *31*, 1835–1841. [CrossRef]